Piezo initiates transient production of collagen IV to repair damaged basement membranes

Aubrie M. Stricker[1], M. Shane Hutson[2], Andrea Page-McCaw[1,3]

[1]Department of Cell and Developmental Biology, Center for Matrix Biology, Program in Developmental Biology, Vanderbilt University, Nashville, TN, USA

[2]Department of Physics and Astronomy, Department of Biological Sciences, Vanderbilt University, Nashville, TN, USA

[3]Lead contact: andrea.page-mccaw@vanderbilt.edu

Summary

Basement membranes are sheets of extracellular matrix separating tissue layers and providing mechanical support. Their mechanical properties are determined largely by their most abundant protein, Collagen IV (Col4). Although basement membranes are repaired after damage, little is known about how. To wit, since basement membrane is extracellular it is unknown how damage is detected, and since Col4 is long-lived it is unknown how it is regulated to avoid fibrosis. Using the basement membrane of the adult *Drosophila* midgut as a model, we show that repair is distinct from maintenance. In healthy conditions, midgut Col4 originates from the fat body, but after damage, a subpopulation of enteroblasts we term “matrix menders” transiently express Col4, and Col4 from these cells is required for repair. Activation of the mechanosensitive channel Piezo is required for matrix menders to upregulate Col4, and the signal to initiate repair is a reduction in basement membrane stiffness. Our data suggests that mechanical sensitivity may be a general property of Col4-producing cells.

Keywords: Basement membrane, *Drosophila*, Collagen IV, midgut, Piezo, matrix, tensional stiffness, enteroblasts, homeostasis, damage, repair

31 **Introduction**

32 Extracellular matrix (ECM) is an essential conserved component of all animal
33 tissues. In addition to providing structural support, ECM influences cell adhesion, shape,
34 signaling, and behaviors. When tissues are damaged, ECM needs to be repaired, and
35 many human diseases have pathological damage to ECM[1]. Despite the critical
36 importance of ECM repair, little is known about these cellular and molecular processes.
37 At the most fundamental level, it is unknown how cells detect ECM damage. Moreover,
38 ECM proteins, including collagens, are among the most stable proteins in the body, with
39 the longest-lived exhibiting half-lives on the order of an animal's lifetime[2]. ECM longevity
40 presents a special challenge, as repairing with too much ECM causes fibrosis. In this
41 study, we identify a mechanism cells use to sense damaged matrix, and they respond
42 by transiently producing matrix until repair is completed.

43 ECM can be subdivided into stromal matrix and basement membrane (basal
44 lamina). Basement membranes, the focus of this study, are the most ancient and
45 conserved ECM, arising along with multicellularity itself[3]. Basement membranes are thin
46 sheets of matrix that underlie epithelia and wrap around muscles and organs. Their
47 most abundant protein is collagen IV (Col4), a heterotrimer that self-assembles *in vitro*
48 into 2D networks and provides structural support[4]. *In vivo*, networks of Col4 are
49 apposed to networks of laminin, and like Col4, laminin self-assembles *in vitro* into a 2D
50 sheet[5]. Self-assembly raises questions about the nature of basement membrane repair.
51 Is there a continuing self-assembly process for maintenance that also functions
52 passively to repair damage? Or is repair an active process, with cells sensing damage
53 and directing repair?

54 *Drosophila* offers an excellent model to address questions of basement
55 membrane homeostasis and repair. Flies have the same basement membrane structure
56 and composition as mammals, with all the main components but fewer copies of each
57 one: one collagen heterotrimer, two laminin heterotrimers, one nidogen gene, and one
58 perlecan gene[6]. The endogenous Col4 a2 (Vkg) has been "trapped" with a GFP exon,
59 generating a functional Vkg-GFP protein, a tremendously powerful reagent for imaging
60 and genetics. To analyze basement membrane repair, we developed the *Drosophila*
61 posterior midgut as a model tissue. The fly gut is a monolayer epithelium derived from
62 stem cells that generate two lineages, enterocytes and enteroendocrine cells, with
63 intermediates in between[7–9]. The gut epithelium is surrounded by peristalsis muscles,
64 and underlying the epithelium and surrounding the muscles are basement membranes
65 (Fig. 1A). When adult flies ingest dextran sodium sulfate (DSS), it gets visibly lodged in
66 the gut basement membrane, damages its structure, and reduces its stiffness[10]. After
67 DSS removal, repair occurs within two days, providing a window for analyzing genetic
68 requirements. How basement membrane repair is regulated in the fly gut, or in any
69 tissue, is unclear.

70 In this study, we find that genes encoding basement membrane components are
71 required for both repair and maintenance of the adult basement membrane. However,
72 after damage, the source of Col4 for the midgut basement membrane changes: without
73 damage, Col4 originates from the fat body, but after damage, local epithelial cells
74 transiently upregulate Col4 and its crosslinking enzyme Peroxidasin. These "matrix
75 mender" cells are specialized enteroblasts, and knocking down Col4 in enteroblasts
76 inhibits gut basement membrane repair. Damage-induced expression of Col4 in matrix

77 mender cells requires the mechanosensitive channel *Piezo*, suggesting they sense and
78 respond to tissue mechanics. Indeed, reducing basement membrane stiffness by
79 reducing collagen crosslinking is sufficient to induce Col4 expression in matrix mender
80 cells in a Piezo-dependent manner. Interestingly, most or all the Col4 in the gut
81 originates from Piezo-expressing cells, suggesting that Piezo-based mechano-
82 regulation may be a general strategy to regulate Col4 production.
83

84 **Results**

85 **Basement membrane repair and maintenance require many of the same**
86 **components.**

87 DSS directly damages the posterior midgut basement membrane of *Drosophila*[10].
88 In brief, after ingestion, DSS is transported through enterocytes to accumulate in the
89 underlying basement membrane (Fig. 1A). This mechanism is different from mice,
90 where the epithelium excludes DSS while it is intact[10,11]. In flies, DSS-containing
91 basement membranes swell, becoming thicker and less dense as assayed by TEM and
92 super resolution microscopy, and losing their tensile stiffness as assayed in a
93 mechanical tensile strain assay[10]. The mechanical damage to the gut basement
94 membranes alters the gut muscle shape. When wrapped by weakened basement
95 membranes, the gut muscles hyper-contract (Fig. 1A, right side). Identical changes to
96 gut muscle shape are observed in animals lacking the Col4 covalent-crosslinking
97 activity of Peroxidasin (Pxn)[10,12,13], and basement membranes from such animals also
98 have reduced tensile stiffness in the mechanical stretching assay[10,13,14]. Thus,
99 basement membrane stiffness can be inferred from gut muscle shape, visible either as
100 outlined by basement membrane (Fig. 1A) or by as stained by actin (Fig. 3F-I). After
101 removing DSS, basement membrane is repaired in two days, restoring both the
102 thickness/structure of the basement membrane itself and the aspect ratio of the
103 muscles[10]. Repair requires basement membrane protein synthesis, including *vkg* and
104 *LanB1*, as well as *Peroxidasin* (*Pxn*), suggesting damaged basement membrane is
105 replaced with new matrix[10].

106 We asked whether other conserved basement membrane proteins were required
107 for repair by targeting Perlecan (*trol*), Nidogen (*Ndg*), and the Col4 extracellular
108 chaperone, *SPARC*. These genes are required for basement membrane assembly
109 during development, so we knocked them down with dsRNA in 6-day old adults, well
110 after adult basement membranes were formed. Knockdown was initiated ubiquitously
111 with *TubP-Gal4* for two days, then flies were fed DSS for two days, then repair was
112 allowed for two days before the guts were fixed and analyzed. Assessing basement
113 membrane function by analyzing muscle shape (aspect ratio), we found *Perlecan/trol*,
114 *Ndg*, and *SPARC* were all required for repair (Fig. 1B-G, Fig. S1A-C).
115 To probe the relationship between repair and maintenance, we asked if these
116 genes were required for basement membrane maintenance, without external damage,
117 by knocking them down for longer. In the repair assay, the undamaged controls showed
118 that *trol*, *Ndg* and *SPARC* were not required for basement membrane maintenance over
119 6 days of knockdown. However, when we knocked down *SPARC*, *trol*, and *Ndg* for 10
120 days, without external damage, the gut muscles were dysmorphic, indicating that all
121 three genes are required for maintaining basement membrane over 10 days in adults
122 (Fig. 1H-M, Fig. S1D-F). In contrast, knocking down non-matrix extracellular proteins
123 *Gbp1* or *Gbp2*[15] had no effect on basement membrane maintenance or repair (Fig.
124 S1G-R). Thus, basement membrane is replaced faster during repair than during normal
125 homeostatic maintenance.
126
127 **Col4 and Peroxidasin are upregulated in some gut cells following damage.**

128 Although basement membranes must be maintained all throughout the body,
129 damage-triggered repair should be a localized process. The Col4 in many *Drosophila*
130 tissues originates from a distant organ, the fat body[16,17], and we found that was true
131 also for the undamaged gut by targeting the GFP moiety in *vkg-GFP/+* heterozygotes.
132 *vkg-GFP/+* gut basement membranes fluorescence (Fig. 2A), but when dsRNA against
133 GFP was expressed in all cells with *TubP-Gal4*, there was virtually no gut fluorescence
134 (Fig. 2B). When GFP was knocked down specifically in the fat body with *c564-Gal4*, gut
135 fluorescence was also extremely low (Fig. 2C,D), suggesting that most of the gut Col4
136 originates from the fat body, a distant rather than local source. Importantly, the
137 untagged *vkg* allele was not affected by this knockdown strategy, and *vkg*
138 heterozygotes are viable and healthy[17], so the gut basement membrane was still
139 functional.

140 To identify a potential local source of Col4 after DSS damage, we used *Cg-Gal4*,
141 where Gal4 is under control of an enhancer that lies between the two head-to-head
142 promoters of Col4a1 and Col4a2, which together form the single fly Col4 heterotrimer.
143 In controls, only a few cells faintly expressed *Cg>GFP* in the gut, but after damage the
144 number of *Cg>GFP* cells in the gut increased dramatically, from 1.8% to 5.7% of gut
145 epithelial cells (Fig. 2E-G). Further, on a per cell basis the level of expression was
146 higher after damage (Fig. 2H). Interestingly, reporters for *Pxn* and *Laminin* (*Pxn>GFP*
147 and *LanB1>GFP*) were active in cells of the gut even without basement membrane
148 damage (Fig. S2), although the number of *Pxn>GFP* cells doubled after damage (Fig.
149 2I,J). We dubbed these *Cg>GFP* cells “matrix menders”. Interestingly, after the gut
150 basement membrane was repaired, matrix menders were not observed (Fig. 2G). Thus,

151 in response to basement membrane damage these cells synthesize new Col4, but
152 synthesis is halted once repair is complete.
153
154 **Lineage tracing indicates matrix menders are a subset of enteroblasts.**
155 To determine the cellular identity of matrix menders, intestinal stem cells were
156 stained with anti-Delta: ~70% of *Cg>GFP* cells were adjacent to stem cells (86/122, see
157 Fig. 3A). This suggested that matrix menders are the daughters of stem cells, either
158 enteroblasts or pre-enteroendocrine (pre-EE) cells. For lineage-tracing, we turned to the
159 Gal4 technique for real-time and clonal expression (G-TRACE)[18]. In this system, "real-
160 time" Col4 expression was reported by *Cg-Gal4* driving *UAS-nlsRFP*, whereas nuclei
161 that previously expressed Col4 ("lineage expression") were permanently labeled with
162 nlsGFP (Fig. 3B). Anti-Prospero, which labels pre-EE and enteroendocrine cells, did not
163 colocalize with either Col4-expressing (RFP+) cells or their lineage (GFP+) (Fig. 3C-
164 C'''). However, the enterocyte-specific antibody Pdm1 stained about a quarter of GFP+
165 cells (Fig. 3D-D''', E-E''') after repair, while almost never labeling RFP+ cells. These
166 results indicate that the matrix menders are enteroblasts, but they stop expressing Col4
167 before differentiating into enterocytes. Enteroblasts are small protrusive cells that
168 migrate away from the stem cells (Fig. 3F,G, and [19]) and are in contact with the
169 basement membrane (Fig. S3A,B), as are the matrix menders (Fig. 3A,H,I). Not all
170 enteroblasts are matrix menders, however: DSS treatment gives rise to ~2.5 times as
171 many enteroblasts labeled with *Su(H)>GFP* than matrix mender cells labeled with
172 *Cg>GFP* (Fig. S3C).
173

174 **Matrix menders are dispensable after repair.**

175 G-TRACE gave insight into the lifespan of matrix mender cells after they stopped
176 expressing collagen. The number of Col4-expressing RFP+ nuclei increased in
177 response to DSS and then declined after repair (Fig. 3J), similar to Cg>GFP cells (Fig.
178 2G), although because nuclear RFP lasts longer than cytoplasmic GFP, more RFP+
179 cells are observed for longer. Contrary to expectations, however, RFP+ cells did not
180 transition into GFP-only lineage-labeled cells: although RFP+ cells increase in number 2
181 days after DSS removal, there is no corresponding delayed pulse of GFP+ lineage
182 label, indicating that most red cells are removed (Fig. 3K). Thus, it appears matrix
183 mender cells are short-lived after they have completed repair.

184

185 **Collagen IV from enteroblasts is required for repair.**

186 We asked whether Col4 synthesized by the matrix menders is required to repair
187 the gut basement membrane by knocking down collagen specifically in enteroblasts and
188 assaying repair. When *Col4a1* was knocked down in enteroblasts with *Su(H)-Gal4*, only
189 29% (n = 7) of the animals repaired their gut basement membranes, indicating that the
190 Col4 from the matrix menders is required for gut basement membrane repair (Fig. 3L).

191

192 **Piezo is required for basement membrane repair and for Col4 upregulation**

193 How does the gut sense damage to turn on Col4? DSS makes basement
194 membranes less stiff[10], and we envision most types of matrix damage would result in
195 reduced stiffness; thus, we reasoned a mechanosensitive mechanism might detect
196 basement membrane damage. Piezo is a mechanosensitive ion channel active in the

197 gut[7,20,21], so we tested its role in basement membrane maintenance and repair. *Piezo*^{KO}
198 null flies are homozygous viable, and the basement membranes in aged *Piezo*^{KO} adult
199 animals appeared healthy (Fig. 4D-F), indicating no role for Piezo in maintenance.
200 However, after feeding them DSS for two days, *Piezo*^{KO} flies were unable to repair their
201 basement membranes (Fig. 4A-C). *Piezo* is the first gene identified required specifically
202 for repair and not maintenance.

203 These results indicate that basement membrane repair is triggered by the
204 presence of damage and detected by a Piezo-based mechanosensitive mechanism. To
205 determine if Piezo was required for local Col4 production in matrix mender cells, we
206 quantified the number of *Cg>GFP* cells in *Piezo*^{KO} versus control midguts after DSS
207 damage. In controls, 5.8% of epithelial midgut cells expressed GFP, but in *Piezo*^{KO} only
208 1.9% expressed GFP (Fig. 4G-I). In addition to having fewer matrix menders, there was
209 a 2.4-fold decrease in *Cg>GFP* expression levels in the *Piezo*^{KO} guts (Fig. 4J). Thus,
210 *Piezo* is required for Col4 upregulation in response to damage.
211

212 **Piezo detects decreased basement membrane stiffness to activate matrix**
213 **menders.**

214 What aspect of basement membrane damage does Piezo respond to? To test
215 the stiffness hypothesis, we altered basement membrane stiffness another way, by
216 inhibiting Pxn crosslinking, known to contribute substantially to basement membrane
217 tensile stiffness[13,14]. Peroxidasin is irreversibly inhibited by Phloroglucinol (PHG), and
218 we previously showed that 100 μm PHG decreases the tensile stiffness (viscoelastic
219 modulus) of adult fly basement membranes by half[13]. PHG-induced decrease in

220 stiffness was evident in the muscle aspect ratio, and even more pronounced with 5 mM
221 PHG (Fig. 4M). Excitingly, 100 μM PHG activated *Cg>GFP* in 3.5% of gut epithelial
222 cells, and 5 mM PHG activated *Cg>GFP* in 5.3%, levels similar to DSS (Fig. 4K-N).
223 Further, stiffness-induced activation of Col4 in matrix menders required *Piezo*, as
224 *Piezo*^{KO} flies had no increase in *Cg>Gal4* cells with PHG (Fig. 4N-P). Without *Piezo*, the
225 levels of reporter expression actually fell in response to PHG (Fig S4A,B). These results
226 indicate that Piezo responds to the reduction in basement membrane stiffness to
227 activate matrix synthesis.
228

229 **Piezo must be activated in Col4-expressing cells for repair to occur.**

230 To determine specifically if Piezo activation was required for repair, we used the
231 inhibitor *Grammostola spatulata* mechanotoxin #4 (GsMTx4) from tarantula toxin, which
232 inserts in the plasma membrane and reduces local membrane tension, inhibiting
233 tension-based activation of Piezo and other mechanosensitive channels[22–24]. Although
234 wild-type GsMTx4 acts non-cell autonomously, the mutant GsMTx4-AP[25] is cell
235 autonomous. We compared the ubiquitous expression of GsMTx4-AP to homozygous
236 *Piezo*^{KO} mutants for their ability to repair after damage. Only 33% of the GsMTx4-AP
237 expressing guts were able to repair (n=12), similar to 22% repair in homozygous
238 *Piezo*^{KO} mutants, indicating that Piezo must be activated for basement membrane repair
239 (Fig. 4Q). Further, repair was completely blocked when GsMTx4-AP was expressed
240 specifically in Cg-expressing cells, yet repair was not impaired at all when GsMTx4-AP
241 was expressed in tracheal cells or neurons, cell types that also express Piezo ([26] and

242 Fig. S4C) and reside in the gut (Fig. 4Q). Thus, basement membrane repair requires
243 Piezo activation specifically in cells that express Col4.
244
245 **Piezo positive cells are the source of Col4.**
246 As an orthogonal approach to analyzing the relationship between Piezo and
247 Col4, we asked whether the collagen from Piezo-expressing cells was incorporated into
248 the basement membrane of the midgut. We knocked down GFP in a heterozygous *Vkg-*
249 *GFP/+* animal, throughout development into adulthood. As expected, ubiquitously
250 knocking down GFP resulted in basement membranes with almost no GFP, both in
251 undamaged and damaged conditions. Interestingly, knocking down GFP with *Piezo-*
252 *Gal4* gave similarly low levels of GFP in gut basement membranes (Fig. 4R-T) –
253 suggesting that all cells that contribute Col4 to the gut also express Piezo. Similar
254 results were found after DSS damage, indicating that both in the absence and presence
255 of damage, midgut Col4 comes from Piezo-expressing cells (Fig. 4T).

256 **Discussion**

257 Using the basement membrane around the *Drosophila* posterior midgut as a
258 model, we find that basement membrane damage is repaired by a distinct set of local
259 cells, matrix mender cells, that respond to basement membrane stiffness to initiate Col4
260 expression. Upregulation of Col4 in matrix menders requires activation of the
261 mechanosensitive channel Piezo. Because Piezo is known to be activated by a
262 reduction in membrane tension[27], our results imply that a reduction in basement
263 membrane stiffness causes stretching of the plasma membrane. The matrix mender
264 cells have a large area of contact with the basement membrane they monitor (Fig. 3H,I),
265 and we envision that when the basement membrane tensional stiffness is reduced – i.e.
266 when the basement membrane stretches more – the plasma membrane of the
267 neighboring cells is also stretched. Contraction of the gut peristalsis muscles would
268 exacerbate membrane stretching in the matrix menders.

269 Lineage tracing indicates that matrix menders are short-lived enteroblasts, with
270 some differentiating into enterocytes and others removed from the population,
271 presumably by dying. Knocking down Col4 specifically in enteroblasts prevented
272 basement membrane repair, confirming that matrix menders are enteroblasts. These
273 cells synthesize collagen for less than two days after DSS removal, consistent with the
274 48 h time frame for repair[10], and lineage tracing indicates they stop producing collagen
275 before they differentiate or die, suggesting that matrix menders are specialized for their
276 function of repairing the matrix. The short duration of collagen expression is important
277 because collagen itself is a long-lived molecule, and too much of it would alter tissue

278 mechanical properties causing fibrosis. Thus, matrix mender cells appear to be
279 exquisitely balanced to produce enough Col4 for repair, but not too much.
280 We speculate that the damage status of many basement membranes may be
281 monitored by Piezo. When Vkg-GFP was knocked down specifically in *Piezo*-expressing
282 cells, the gut basement membranes incorporated little Vkg-GFP, even the undamaged
283 ones that get Col4 from the fat body. These data indicate that fat body cells also
284 express Piezo. Like matrix mender cells in the gut, fat body cells are in contact with a
285 local basement membrane[28,29]. These results raise the possibility of a general model
286 that collagen-producing cells use a Piezo-dependent mechanism for
287 mechanosensitivity. In support of this concept, we previously observed that when Col4
288 crosslinking is inhibited in larvae, the whole-body levels of Col4 are increased (McCall
289 et al, Fig S7), a result that supports the idea that Col4 levels respond to of basement
290 membrane stiffness.
291

292 **Acknowledgements**

293 We thank K. Elkie Peebles, Kimberly LaFever, Jordyn Sanner Barr, and Leah Caplan
294 for technical help and Barry Denholm, BDSC, VDRC, and Kyoto *DSC* for fly stocks.
295 Anti-Pdm1 was a gift from Yang Xiaohang. Work was supported by NIGMS
296 (R01GM137595 to A.P-M., and F31GM148021 to A.S.)
297

298 **Author Contributions**

299 AS: Conceptualization, methodology, validation, formal analysis, investigation,
300 resources, writing and editing, visualization. MSH: Methodology, software. APM:

Conceptualization, methodology, writing and editing, visualization, supervision, project administration.

Competing interests

The authors declare no competing interests.

306 **Figure Legends**

307 **Figure 1. Adult basement membrane repair and maintenance require new matrix**
308 **components.**

309 **(A) Left: *Drosophila* midgut.** The gut tube is enclosed by peristalsis muscles
310 (magenta), each wrapped in basement membrane (green). Inside the muscle layer, the
311 gut monolayer epithelium (blue nuclei/DAPI stain) comprises absorptive enterocytes
312 (light blue), stem cells (brown), enteroblasts (dark blue), and pre-EE and EE cells
313 (orange), all siting on basement membrane continuous with muscle basement
314 membrane (green).

315 **Right: DSS damage.** DSS (orange dots) is ingested, transported through the
316 enterocytes, and deposited in the underlying basement membrane where it causes
317 damage, making basement membrane less dense and less stiff, resulting in visibly
318 dysmorphic muscles. Basement membranes and muscle shapes are fully repaired 2 d
319 after DSS is removed. For details see Howard et al., (2019). Micrograph bars, 10 μm.

320 **(B-G)** *trol* and *Ndg* are required for basement membrane repair in adult guts. Damage is
321 quantified as muscle shape. Mean +/- SEM, significance evaluated by ANOVA. Bar, 10
322 μm.

323 **(H-M)** *trol* and *Ndg* are required for basement membrane maintenance without external
324 damage in adult guts. Significance evaluated by *t*-test.

325

326

327 **Figure 2. "Matrix mender" gut cells upregulate Col4 after basement membrane**
328 **damage.**

329 **(A-D)** In undamaged conditions, midgut Col4 comes from the fat body. Surface view of
330 gut basement membrane in *Vkg-GFP/+* controls (A). Ubiquitous knockdown of GFP
331 eliminated Vkg-GFP fluorescence in the gut (B). Similar fluorescence loss was observed
332 with fat-body specific GFP knockdown, using *c564-Gal4* (C,D). Bar, 10 μm.
333 **(E-H)** Col4 transcriptional reporter, *Cg-Gal4,* was activated in unknown epithelial cells
334 (matrix menders) of the posterior midgut in response to DSS-induced basement
335 membrane damage (E-F). *Cg>GFP* expression stops after repair, 2 d after DSS removal
336 (G). DSS increases both the number of Cg-expressing cells (G), and the intensity of
337 expression (H). Bar, 20 μm. Significance evaluated by ANOVA in G and *t*-test in H.
338 **(I,J)** Peroxidasin transcriptional reporter, *pxn-Gal4*, was activated in some epithelial
339 cells of the posterior midgut in response to DSS-induced basement membrane damage,
340 appearing similar to *Cg-Gal4* expressing cells. Bar, 20 μm.
341
342 **Figure 3. Matrix menders are enteroblasts that provide Col4 necessary for repair**
343 **and die soon after repair is completed.**
344 **(A)** *Cg>GFP* matrix mender cells localized near but not with Delta-labeled intestinal
345 stem cells. Bar, 20 μm.
346 **(B)** Overview of *Gal4* technique for real-time and clonal expression (G-TRACE).
347 Adapted from Evans et al., 2009.
348 **(C-E)** *Cg>G-TRACE* real-time expressing cells (red) and lineage expressing cells
349 (green). *Cg>G-TRACE* cells did not colocalize with the EE/pre-EE labeled with anti-
350 Prospero (C). Some *Cg>G-TRACE* cells colocalized with enterocytes labeled with anti-
351 Pdm1 after 2d recovery from DSS (D - No recovery, E - 2 d recovery). Bar, 10 μm.

352 **(F-I)** Enteroblasts (F-G) and matrix mender cells (H-I) have extensive contact with
353 basement membrane, both with and without DSS. Actin staining labels muscles
354 wrapped in basement membrane. Bar, 10 μm.
355 **(J,K)** After DSS damage and repair, most *Cg>G-TRACE* real-time expressing cells (red,
356 J) do not transition into GFP-only lineage expressing cells (green, K), indicating that Cg-
357 expressing cells are lost from the epithelium after repair. All real-time expressing cells
358 (red) whether or not they were also lineage labeled (green) are shown in J; only green-
359 labeled cells, not red, are shown in K. Together, panels J and K represent each cell only
360 once.
361 **(L)** Col4 from enteroblasts is required for repair. Percentage of guts with healthy
362 basement membrane morphology when *Col4a1* was knocked down in enteroblasts
363 using *Su(H)-Gal4*. Flies were fed DSS or not, followed by 2 d of recovery. Morphology
364 was assessed on a per-gut basis by the muscle shape and scored blinded to sample
365 identity.
366
367 **Figure 4. Piezo is required for basement membrane repair, by activating Col4**
368 **synthesis in the matrix mender cells.**
369 **(A-F)** *Piezo* is required for basement membrane repair in adult guts, assayed 2 d after
370 removing DSS, but not required for basement membrane maintenance, assayed in
371 aged 10 d *Piezo*^{KO} adults with no external damage. Basement membrane and muscle
372 shape visualized by Vkg-GFP. Mean +/-SEM. Significance evaluated by ANOVA (C) or
373 *t-test* (F). Bar, 10 μm.

374 **(G-J)** *Piezo* is required for matrix mender cells to express Col4 (*Cg>GFP*) in response
375 to DSS damage. The number of Col4-expressing cells (*Cg>GFP)* and the level of
376 expression were both significantly reduced in *Piezo*^{KO} flies. Significance evaluated by
377 ANOVA (I) and *t-test* (J). Bar, 20 µm.
378 **(K-P)** The crosslinking inhibitor PHG reduced basement membrane stiffness, evidenced
379 by dysmorphic muscles (M) and tensile stiffness measurements (Peebles et al, 2023).
380 PHG-induced changes to membrane stiffness activated matrix mender cells (K,L,N), in
381 a Piezo-dependent manner (N-P) Significance evaluated by ANOVA. Bar, 20 µm.
382 **(Q)** *Piezo* is required in Col4-expressing cells for basement membrane repair. Piezo
383 activity was inhibited in indicated cell populations with GsMTx4. Flies were fed DSS or
384 not for 2 d, followed by 2 d of recovery. Repair was assessed on a per-gut basis by the
385 muscle shape and scored blinded to sample identity.
386 **(R-T)** Even without damage, Col4 in the gut basement membrane is synthesized in cells
387 that also express *Piezo*. Surface view of *Vkg-GFP/+* heterozygous control guts (R,S);
388 Vkg-GFP levels are almost undetectable when GFP is knocked down with *Piezo-Gal4*
389 (S,T). Bar, 20 µm. Significance evaluated by ANOVA.

390

391 **Materials and Methods**

392 **Fly husbandry**

393 Flies were maintained on cornmeal-molasses food at 25° C unless otherwise
394 specified. For temperature-sensitive RNAi studies under *Gal80^{ts}* control, flies were
395 maintained at 18° C until they eclosed. Female flies were then aged at 18° C until they
396 were 6-day adults (mated) before moving them to 29° C to activate the Gal4. Fly stocks
397 used were:

398

Genotype	**Source**
VkgGFP^{791}; tubGal4, tubGal80/S-T	this study
UAS-Nidogen^{RNAi}	VDRC 109625
UAS-Perlecan^{RNAi}	VDRC 105502
UAS-SPARC^{RNAi}	BSC 40885
UAS-Gbp1^{RNAi}	VDRC KK168755
UAS-Gbp2^{RNAi}	VDRC GD16696
UAS-GFP	BSC 1522
UAS-mCD8 GFP	Kyoto 108068
Cg-Gal4	BSC 7011
Pxn-Gal4/TM3	BSC 22805
LanB1-Gal4/CyO	BSC 63941
UAS-Stinger	Cory Evans
VkgGFP^{791}	Carnegie Protein trap library, CC00971
Piezo^{KO}	BSC 58770
Piezo^{KO}, Cg-Gal4/CyO	this study
Piezo^{KO}; UAS-GFP/TM3	this study
Piezo^{KO}, VkgGFP^{791}	this study
w^{1118}	Todd Laverty, Janelia Farm
UAS-GsMTx4 (active peptide)	Denholm Lab
Elav-Gal4	BSC 8765
Btl-Gal4	Greg Beitel
VkgGFP, UAS-GFP^{RNAi}/CyO, mCh	BSC 9330
Tubulin-Gal4	Kyoto 108069
Piezo-Gal4	BSC 59266
UAS-Piezo^{RNAi}	VDRC 2796

UAS-Cg25c^{RNAi}	VDRC 28369
Su(H)Gal4, UAS-mCD8GFP	BSC 87733

399 **DSS feeding**

400 As described in Amcheslavsky et al. (2009) and Howard et al. (2019), a 2.5 cm x
401 3 cm piece of chromatography paper (Whatman 3030-861, Grade 3 MM CHR) was
402 placed in an empty vial. 500 µl of a 5% sucrose solution with or without 3% 36-50 kDa
403 DSS (dextran sulfate sodium salt colitis grade, MP Biomedicals, CAS number 9011-18-
404 1, 36,000 – 50,000 MW) was added to the paper in the vial. Flies utilizing the Gal80^{ts}
405 system were moved to 29° C for 2 days to ensure the Gal4 was active prior to starting
406 DSS feeding treatments. Flies not utilizing the Gal80^{ts} system were aged 3-5 days at
407 25° C prior to starting DSS feeding treatments. Female flies were anesthetized and
408 carefully placed in the vial to ensure they did not contact the liquid. Flies were added to
409 new vials with fresh media each day for 2 days. For recovery experiments, flies were
410 transferred to a vial containing standard cornmeal-molasses food for 2 days. For
411 imaging in 3 dimensions (Z-stacks), flies on standard cornmeal-molasses food were fed
412 5% sucrose for 4 hours before dissection to reduce autofluorescence from the food.

413 **Phloroglucinol feeding**

414 Non-cornmeal molasses food was freshly made with or without 100 µM or 5 mM
415 Phloroglucinol (PHG) (Sigma-Aldrich, CAS number 108-73-6) and solidified in a vial
416 overnight. 20 aged female flies and 5 male flies were added to the vials with or without
417 PHG. Flies were kept at 25° C for 5 days. Prior to dissection, flies were fed 5% sucrose
418 for 4 hours before dissection to reduce autofluorescence from the food.

419 **CNA35 staining**

420 Immediately after gut dissections, CNA35 green monomer (1:100) was added to
421 guts for 2 hours, followed by a 1 hour fixation with 8% PFA.

422 **Gut dissections and preparations**

423 Adult females were placed in cold Grace's media and pinched between the
424 abdomen and thorax using sharp #5 dissecting forceps (Dunmont). The abdomen was
425 separated from the thorax, and the integument surrounding the abdomen was peeled
426 away, exposing the gut and Malpighian tubules, being careful not to pinch or stretch the
427 gut. The Grace's media was removed using a Pasteur pipette, followed by one quick
428 wash with 1x PBS (137 mM NaCl, 2.7 mM KCl, 10 mM Na_2HPO_4, and 1.8 mM KH_2PO_4).
429 The guts were fixed with 4% paraformaldehyde (Ted Pella, Paraformaldehyde 16%,
430 Product #18505) in PBS for 20 minutes at room temperature, or 8% paraformaldehyde
431 in PBS for 60 minutes at room temperature, followed by 3 quick washes in PBS, and 4 x
432 15 min washes with PBS or PBT.

433 For immunofluorescence experiments, blocking buffer was added to fixed guts
434 for 2 hours at room temperature or overnight at 4° C then incubated in primary antibody
435 and 0.2 μM SiRActin (Spirochrome Cat# SC001) in PBS or PBT overnight at 4° C,
436 followed by 4 x 30 min washes with 1x PBS. Secondary antibodies were added for 2
437 hours at room temperature, followed by 4 x 30 min washes. Guts were then mounted in
438 DAPI-containing mounting media (Vectashield, Vector Laboratories, H1200). Antibodies
439 used were:

440 - Rabbit anti-GFP (1:200, Torrey Pines, TP401)
441 - Mouse IgG1 anti-Delta (1:50, DSHB SA4)
442 - Mouse IgG1 anti-Prospero (1:50, DSHB MR1A)

443 • Rabbit anti-Pdm1 (1:1000, gift from Yang Xiaohang)
444 • Cy3 goat anti-mouse IgG1 (1:200, Jackson ImmunoResearch Laboratory Inc.)
445 • Cy3 donkey anti-rabbit (1:200, Jackson ImmunoResearch Laboratory Inc.)
446 • Cy5 goat anti-mouse 1gG1 (1:200, Jackson ImmunoResearch Laboratory Inc.)
447 • Cy5 donkey anti-rabbit (1:200, Jackson ImmunoResearch Laboratory Inc.)
448

449 **Light Microscopy**

450 Single optical sections of the guts were imaged using a Zeiss Apotome mounted
451 to an Axio Image M2 with a 63x/1.4 oil Plan-Apochromat objective. Z-stacks were
452 acquired using a 40x/1.3 oil Plan-Apochromat objective at a 0.75 μm step size taken
453 through the top half of the gut tube (lumen through the top of the circumferential muscle
454 layer). Images were taken using an AxioCam MRm camera (Zeiss), X-Cite 120Q light
455 source (Excelitas Technologies), and AxioVision 4.8 software. ImageJ (version 1.53v,
456 National Institutes of Health) 16-bit, ZVI files were used for analysis and figures for
457 images.

458 The fluorescence intensity of the basement membrane was determined by taking
459 single optical slices *en face* through the middle of the circumferential muscles to ensure
460 the same plane of the basement membrane was imaged, and the exposures were kept
461 the same. The fluorescence intensity of the basement membrane was measured in
462 ImageJ using the “box” tool to measure the average intensity of 3 representative regions
463 of the gut basement membrane. Similarly, the background intensity was determined by
464 subtracting the average of 3 boxes outside of the gut region. An AVOVA test was
465 performed (GraphPad Prism 9.5).

466 Fluorescence intensity measurements of gut cells to be compared were acquired
467 at the same exposure from at least 3 experiments done on different days. Maximum
468 intensity projections were created using ImageJ and the line tool was used to draw
469 through the center of the 3 brightest nuclei in the GFP channel and the fluorescence
470 intensity was measured and averaged. Background fluorescence was subtracted by
471 taking the average intensity of 3 lines within the gut region that did not overlap with GFP
472 nuclei. A *t-test* was performed.
473

474 **Measurement of muscle shape**

475 Individual muscle cells were identified and segmented using the software
476 Seedwater Segmenter (Mashburn et al. 2012). Custom code in Mathematica (Wolfram
477 Inc., Champaign, IL) was then used to analyze the segmented images and determine
478 the aspect ratio of each muscle cell.
479

480 **Quantifying number of cells**

481 GFP+ cells were manually quantified by creating a maximum intensity projection
482 and confirmed by the presence of a nucleus. The total number of nuclei in the posterior
483 midgut was quantified by creating a maximum intensity projection and setting a
484 threshold to select the DAPI-stained nuclei. Images were “despeckled,” and a
485 watershed was applied to the image. Using the ImageJ “analyze particle” feature, the
486 number of particles larger than 10 μm^2 was quantified. The areas where nuclei were
487 fused together or unable to be accurately quantified by ImageJ were manually
488 quantified.

489 **References**

490 1. Iozzo, R.V., and Gubbiotti, M.A. (2018). Extracellular matrix: The driving force of
491 mammalian diseases. Matrix Biology *71–72*, 1–9. 10.1016/j.matbio.2018.03.023.

492 2. Liu, P., Xie, X., and Jin, J. (2020). Isotopic Nitrogen-15 Labeling of Mice Identified
493 Long-lived Proteins of the Renal Basement Membranes. Scientific Reports *10*, 1–7.
494 10.1038/s41598-020-62348-6.

495 3. Fidler, A.L., Vanacore, R.M., Chetyrkin, S.V., Pedchenko, V.K., Bhave, G., Yin, V.P.,
496 Stothers, C.L., Rose, K.L., McDonald, W.H., Clark, T.A., et al. (2014). A unique
497 covalent bond in basement membrane is a primordial innovation for tissue evolution.
498 Proceedings of the National Academy of Sciences of the United States of America
499 *111*, 331–336. 10.1073/pnas.1318499111.

500 4. Yurchenco, P.D., and Furthmayr, H. (1984). Self-Assembly of Basement Membrane
501 Collagen. Biochemistry *23*, 1839–1850. 10.1021/bi00303a040.

502 5. Yurchenco, P.D., Tsilibary, E.C., Charonis, A.S., and Furthmayr, H. (1986). Models
503 for the self-assembly of basement membrane. Journal of Histochemistry and
504 Cytochemistry *34*, 93–102. 10.1177/34.1.3510247.

505 6. Ramos-Lewis, W., and Page-McCaw, A. (2019). Basement membrane mechanics
506 shape development: Lessons from the fly. Matrix Biology *75–76*, 72–81.
507 10.1016/j.matbio.2018.04.004.

508 7. He, L., Si, G., Huang, J., Samuel, A.D.T., and Perrimon, N. (2018). Mechanical
509 regulation of stem cell differentiation through stretch-activated Piezo channel.
510 Nature *555*, 103–106. 10.1038/nature25744.

511 8. Martin, J.L., Sanders, E.N., Moreno-Roman, P., Koyama, L.A.J., Balachandra, S.,
512 Du, X., and O'Brien, L.E. (2018). Long-term live imaging of the Drosophila adult
513 midgut reveals real-time dynamics of division, differentiation and loss. eLife *7*.
514 10.7554/ELIFE.36248.

515 9. Micchelli, C.A., and Perrimon, N. (2006). Evidence that stem cells reside in the adult
516 Drosophila midgut epithelium. Nature *439*, 475–479. 10.1038/nature04371.

517 10. Howard, A.M., Lafever, K.S., Fenix, A.M., Scurrah, C.R., Lau, K.S., Burnette, D.T.,
518 Bhave, G., Ferrell, N., and Page-McCaw, A. (2019). DSS-induced damage to
519 basement membranes is repaired by matrix replacement and crosslinking. Journal
520 of Cell Science *132*. 10.1242/jcs.226860.

521 11. Shimshoni, E., Adir, I., Afik, R., Solomonov, I., Shenoy, A., Adler, M., Puricelli, L.,
522 Sabino, F., Savickas, S., Mouhadeb, O., et al. (2021). Distinct extracellular–matrix
523 remodeling events precede symptoms of inflammation. Matrix Biology *96*, 47–68.
524 10.1016/j.matbio.2020.11.001.

525 12. McCall, A.S., Cummings, C.F., Bhave, G., Vanacore, R., Page-Mccaw, A., and
526 Hudson, B.G. (2014). Bromine is an essential trace element for assembly of
527 collagen IV scaffolds in tissue development and architecture. Cell *157*, 1380–1392.
528 10.1016/j.cell.2014.05.009.

529 13. Peebles, K.E., LaFever, K.S., Page-McCaw, P.S., Colon, S., Wang, D., Stricker,
530 A.M., Ferrell, N., Bhave, G., and Page-McCaw, A. (2024). Peroxidasin is required for
531 full viability in development and for maintenance of tissue mechanics in adults.
532 Matrix Biology *125*, 1–11. 10.1016/j.matbio.2023.11.005.

533 14. Bhave, G., Colon, S., and Ferrell, N. (2017). The sulfilimine cross-link of collagen IV
534 contributes to kidney tubular basement membrane stiffness. American Journal of
535 Physiology - Renal Physiology *313*, F596–F602. 10.1152/ajprenal.00096.2017.

536 15. O'Connor, J.T., Stevens, A.C., Shannon, E.K., Akbar, F.B., LaFever, K.S.,
537 Narayanan, N.P., Gailey, C.D., Hutson, M.S., and Page-McCaw, A. (2021).
538 Proteolytic activation of Growth-blocking peptides triggers calcium responses
539 through the GPCR Mthl10 during epithelial wound detection. Developmental Cell *56*,
540 2160-2175.e5. 10.1016/j.devcel.2021.06.020.

541 16. Pastor-Pareja, J.C., and Xu, T. (2011). Shaping Cells and Organs in Drosophila by
542 Opposing Roles of Fat Body-Secreted Collagen IV and Perlecan. Developmental
543 Cell *21*, 245–256. 10.1016/j.devcel.2011.06.026.

544 17. Ramos-Lewis, W., LaFever, K.S., and Page-McCaw, A. (2018). A scar-like lesion is
545 apparent in basement membrane after wound repair in vivo. Matrix Biology *74*, 101–
546 120. 10.1016/j.matbio.2018.07.004.

547 18. Evans, C.J., Olson, J.M., Ngo, K.T., Kim, E., Lee, N.E., Kuoy, E., Patananan, A.N.,
548 Sitz, D., Tran, P.T., Do, M.T., et al. (2009). G-TRACE: Rapid Gal4-based cell
549 lineage analysis in Drosophila. Nature Methods *6*, 603–605. 10.1038/nmeth.1356.

550 19. Antonello, Z.A. (2015). Robust intestinal homeostasis relies on cellular plasticity in
551 enteroblasts mediated by miR-8–Escargot switch. The EMBO Journal *34*, 2025–
552 2041. 10.15252/embj.201591517.

553 20. Min, S., Oh, Y., Verma, P., Whitehead, S.C., Yapici, N., Van Vactor, D., Suh, G.S.B.,
554 and Liberles, S.D. (2021). Control of feeding by piezo-mediated gut
555 mechanosensation in Drosophila. eLife *10*, 1–30. 10.7554/eLife.63049.

556 21. Lee, J., Cabrera, A.J.H., Nguyen, C.M.T., and Kwon, Y.V. (2020). Dissemination of
557 Ras V12-transformed cells requires the mechanosensitive channel Piezo. Nature
558 Communications *11*, 1–13. 10.1038/s41467-020-17341-y.

559 22. Suchyna, T.M., Johnson, J.H., Hamer, K., Leykam, J.F., Gage, D.A., Clemo, H.F.,
560 Baumgarten, C.M., and Sachs, F. (2000). Identification of a peptide toxin from
561 Grammostola spatulata spider venom that blocks cation-selective stretch-activated
562 channels. Journal of General Physiology *115*, 583–598. 10.1085/jgp.115.5.583.

563 23. Suchyna, T.M., Tape, S.E., Koeppe, R.E., Andersen, O.S., Sachs, F., and Gottlieb,
564 P.A. (2004). Bilayer-dependent inhibition of mechanosensitive channels by
565 neuroactive peptide enantiomers. Nature *430*, 235–240. 10.1038/nature02743.

566 24. Bae, C., Sachs, F., and Gottlieb, P.A. (2011). The Mechanosensitive Ion Channel
567 Piezo1 is Inhibited by the Peptide GsMTx4. Biochemistry *50*, 6295–6300.
568 10.1021/bi200770q.

569 25. Beqja, D., Haidar, S., Nikolaev, M., Shen, Y., and Denholm, B. (2020). Transgenic
570 Tarantula Toxin: A novel tool to study mechanosensitive ion channels in Drosophila.
571 Journal of Insect Physiology *127*, 104116. 10.1016/j.jinsphys.2020.104116.

572 26. Song, Y., Li, D., Farrelly, O., Miles, L., Li, F., Kim, S.E., Lo, T.Y., Wang, F., Li, T.,
573 Thompson-Peer, K.L., et al. (2019). The Mechanosensitive Ion Channel Piezo
574 Inhibits Axon Regeneration. Neuron *102*, 373-389.e6.
575 10.1016/j.neuron.2019.01.050.

576 27. Coste, B., Xiao, B., Santos, J.S., Syeda, R., Grandl, J., Spencer, K.S., Kim, S.E.,
577 Schmidt, M., Mathur, J., Dubin, A.E., et al. (2012). Piezo proteins are pore-forming
578 subunits of mechanically activated channels. Nature *483*, 176–181.
579 10.1038/nature10812.

580 28. Dai, J., Ma, M., Feng, Z., and Pastor-Pareja, J.C. (2017). Inter-adipocyte Adhesion
581 and Signaling by Collagen IV Intercellular Concentrations in Drosophila. Current
582 Biology *27*, 2729-2740.e4. 10.1016/j.cub.2017.08.002.

583 29. Shahab, J., Baratta, C., Scuric, B., Godt, D., Venken, K.J.T., and Ringuette, M.J.
584 (2015). Loss of SPARC dysregulates basal lamina assembly to disrupt larval fat
585 body homeostasis in Drosophila melanogaster. Developmental Dynamics *244*, 540–
586 552. 10.1002/dvdy.24243.

587

Graphical abstract

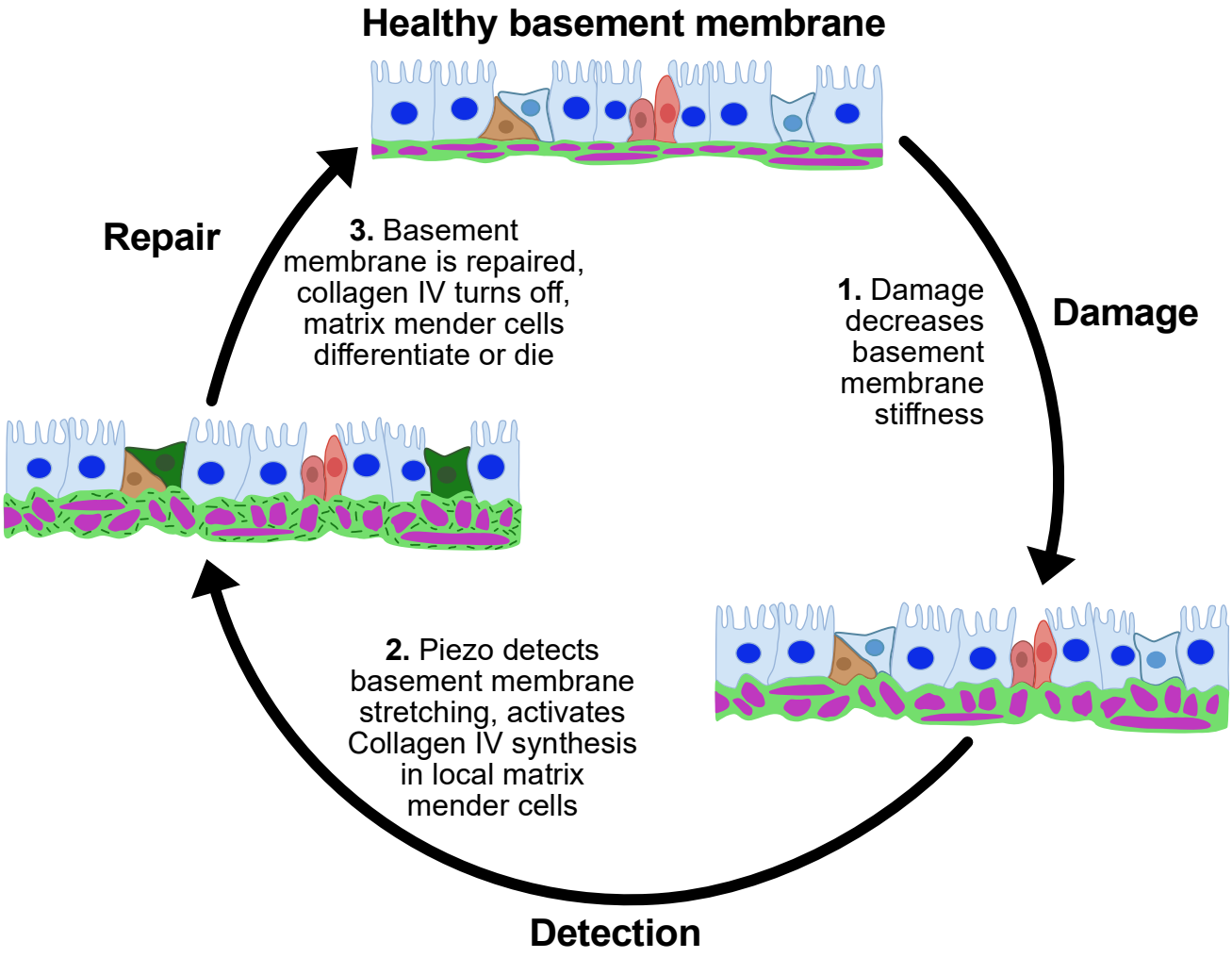

Figure 1

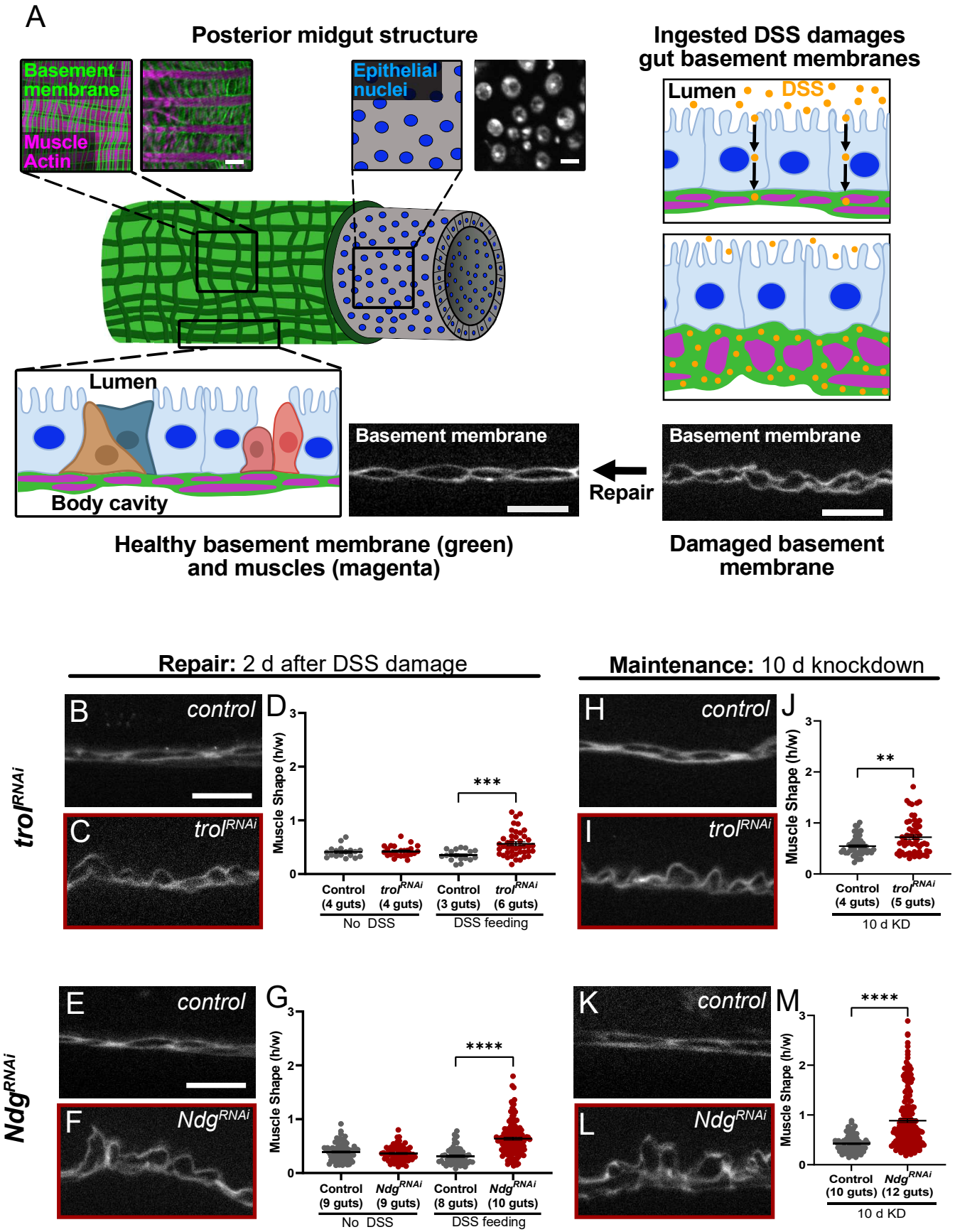
A
Posterior midgut structure
Basement membrane
Muscle Actin
Epithelial nuclei
Lumen
Body cavity
Basement membrane
Healthy basement membrane (green) and muscles (magenta)
Ingested DSS damages gut basement membranes
Lumen
DSS
Basement membrane
Repair
Damaged basement membrane
Repair: 2 d after DSS damage
Maintenance: 10 d knockdown
trolRNAi
B control
C trolRNAi
D
Muscle Shape (h/w)
***
Control (4 guts)
trolRNAi (4 guts)
Control (3 guts)
trolRNAi (6 guts)
No DSS
DSS feeding
H control
I trolRNAi
J
**
Control (4 guts)
trolRNAi (5 guts)
10 d KD
NdgRNAi
E control
F NdgRNAi
G
****
Control (9 guts)
NdgRNAi (9 guts)
Control (8 guts)
NdgRNAi (10 guts)
K control
L NdgRNAi
M
****
Control (10 guts)
NdgRNAi (12 guts)

Figure 2

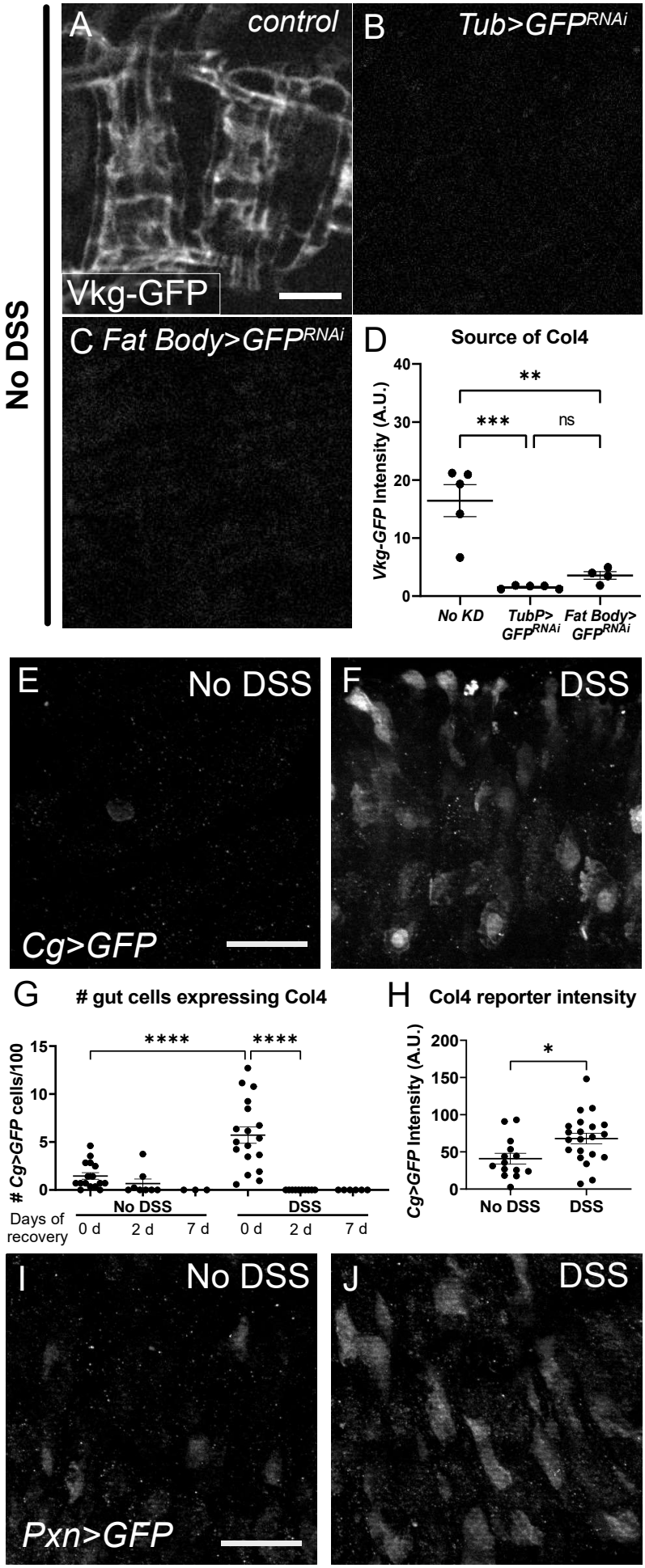
A
control
Vkg-GFP
B
Tub>GFP^RNAi
C Fat Body>GFP^RNAi
No DSS
D
Source of Col4
Vkg-GFP Intensity (A.U.)
40
30
20
10
0
**
***
ns
No KD
TubP> GFP^RNAi
Fat Body> GFP^RNAi
E
No DSS
Cg>GFP
F
DSS
G
gut cells expressing Col4
Cg>GFP cells/100
15
10
5
0
****
****
No DSS
DSS
Days of recovery
0 d
2 d
7 d
0 d
2 d
7 d
H
Col4 reporter intensity
Cg>GFP Intensity (A.U.)
200
150
100
50
0
*
No DSS
DSS
I
No DSS
Pxn>GFP
J
DSS

Figure 3

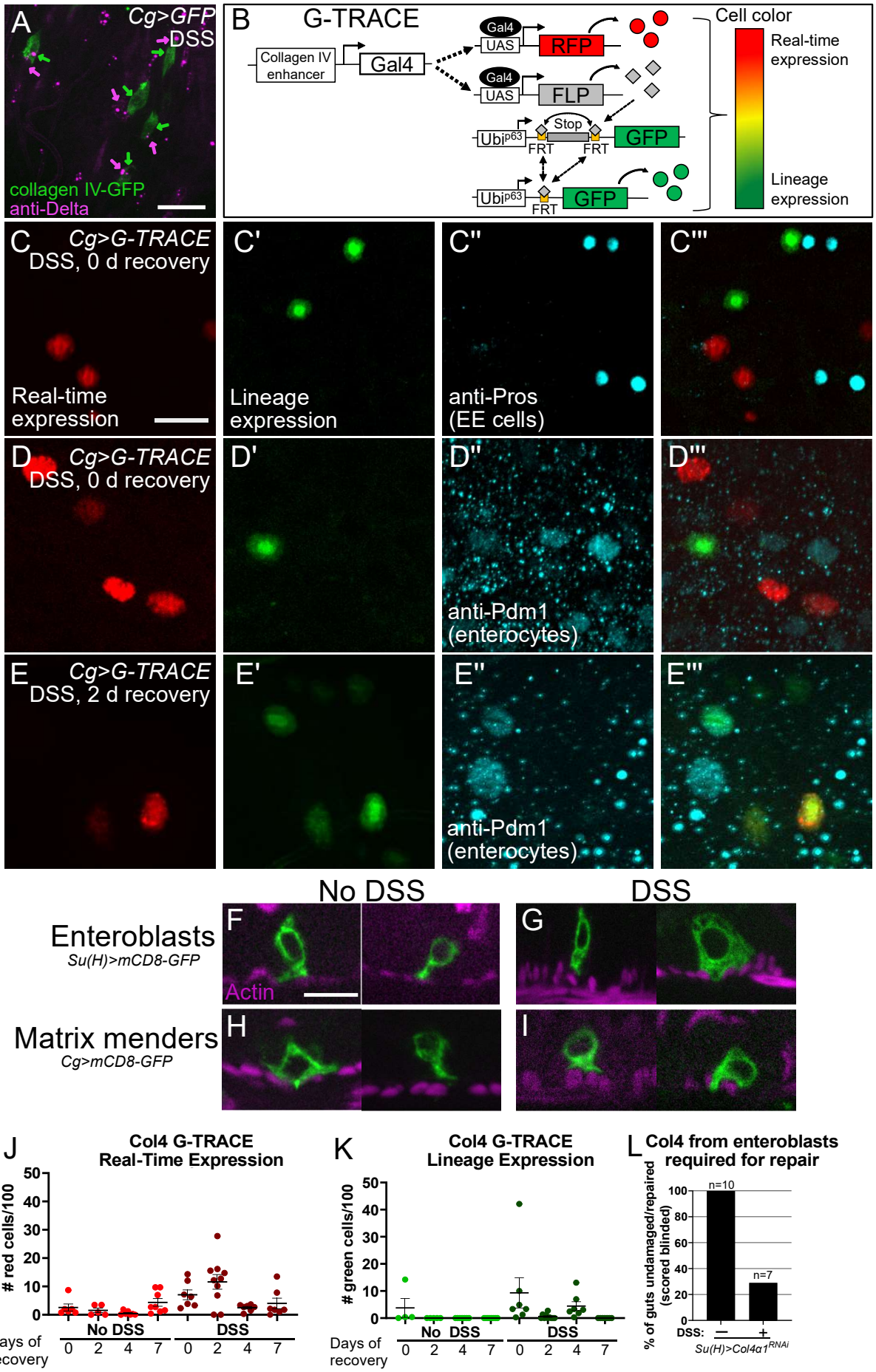
A
Cg>GFP
DSS
collagen IV-GFP
anti-Delta
B
G-TRACE
Collagen IV enhancer
Gal4
Gal4
UAS
RFP
Gal4
UAS
FLP
Stop
Ubi^{p63}
FRT
FRT
GFP
Ubi^{p63}
FRT
GFP
Cell color
Real-time expression
Lineage expression
C
Cg>G-TRACE
DSS, 0 d recovery
Real-time expression
C'
Lineage expression
C''
anti-Pros (EE cells)
C'''
D
Cg>G-TRACE
DSS, 0 d recovery
D'
D''
anti-Pdm1 (enterocytes)
D'''
E
Cg>G-TRACE
DSS, 2 d recovery
E'
E''
anti-Pdm1 (enterocytes)
E'''
No DSS
DSS
Enteroblasts
Su(H)>mCD8-GFP
F
Actin
G
Matrix menders
Cg>mCD8-GFP
H
I
J
Col4 G-TRACE
Real-Time Expression
red cells/100
50
40
30
20
10
0
No DSS
DSS
Days of recovery
0 2 4 7 0 2 4 7
K
Col4 G-TRACE
Lineage Expression
green cells/100
50
40
30
20
10
0
No DSS
DSS
Days of recovery
0 2 4 7 0 2 4 7
L
Col4 from enteroblasts required for repair
% of guts undamaged/repaired (scored blinded)
100
80
60
40
20
0
n=10
n=7
DSS: – +
Su(H)>Col4α1^{RNAi}

Figure 4

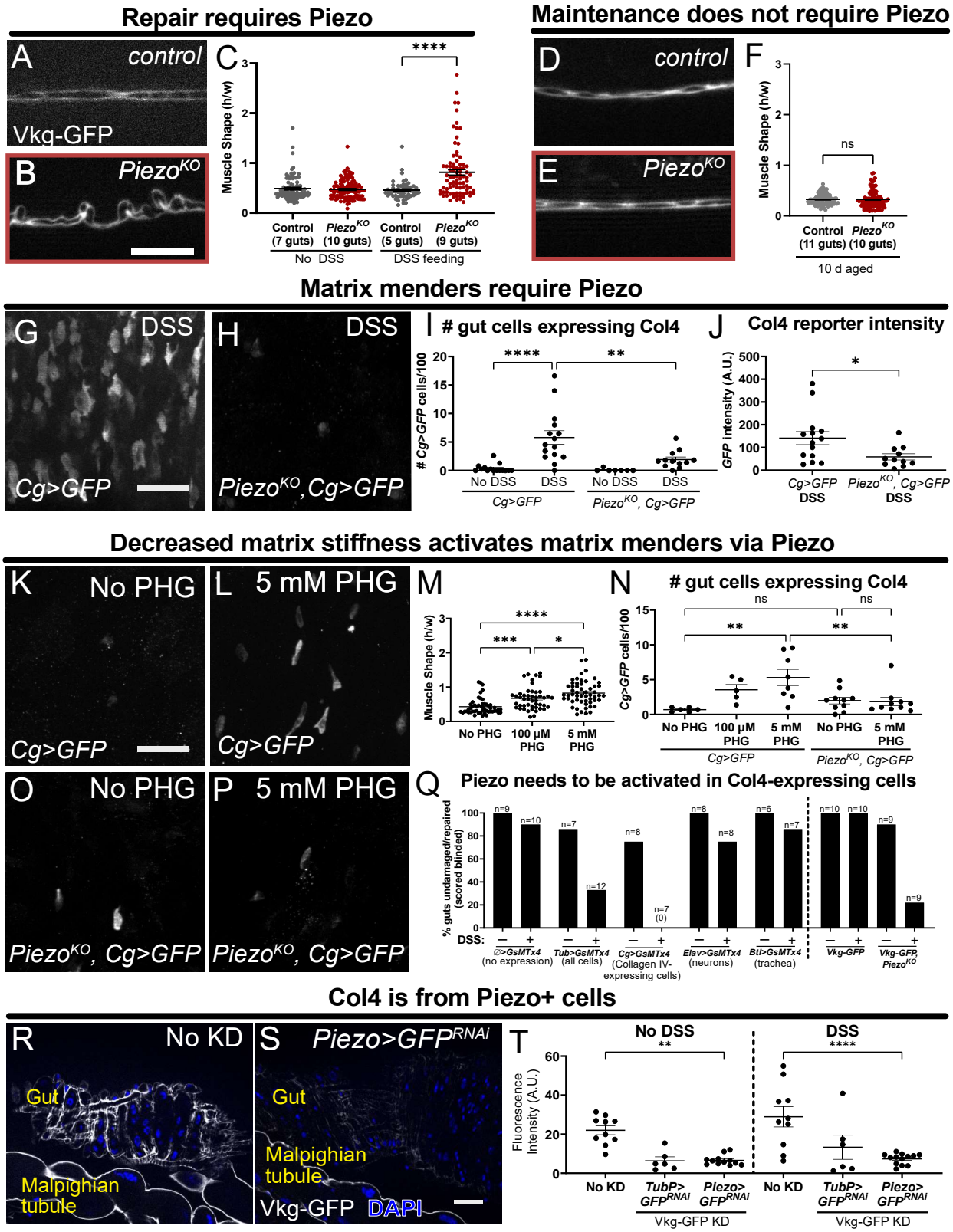
Repair requires Piezo
Maintenance does not require Piezo
A control
Vkg-GFP
B PiezoKO
C
Muscle Shape (h/w)
****
Control (7 guts)
PiezoKO (10 guts)
Control (5 guts)
PiezoKO (9 guts)
No DSS
DSS feeding
D control
E PiezoKO
F
ns
Control (11 guts)
PiezoKO (10 guts)
10 d aged
Matrix menders require Piezo
G DSS
Cg>GFP
H DSS
PiezoKO,Cg>GFP
I # gut cells expressing Col4
Cg>GFP cells/100
****
**
No DSS
DSS
Cg>GFP
PiezoKO, Cg>GFP
J Col4 reporter intensity
GFP intensity (A.U.)
*
Cg>GFP DSS
PiezoKO, Cg>GFP DSS
Decreased matrix stiffness activates matrix menders via Piezo
K No PHG
Cg>GFP
L 5 mM PHG
Cg>GFP
M
Muscle Shape (h/w)
****
***
*
No PHG
100 µM PHG
5 mM PHG
N # gut cells expressing Col4
Cg>GFP cells/100
ns
ns
**
**
No PHG
100 µM PHG
5 mM PHG
No PHG
5 mM PHG
Cg>GFP
PiezoKO, Cg>GFP
O No PHG
PiezoKO, Cg>GFP
P 5 mM PHG
PiezoKO, Cg>GFP
Q Piezo needs to be activated in Col4-expressing cells
% guts undamaged/repaired (scored blinded)
DSS:
∅>GsMTx4 (no expression)
Tub>GsMTx4 (all cells)
Cg>GsMTx4 (Collagen IV-expressing cells)
Elav>GsMTx4 (neurons)
Btl>GsMTx4 (trachea)
Vkg-GFP
Vkg-GFP, PiezoKO
Col4 is from Piezo+ cells
R No KD
Gut
Malpighian tubule
S Piezo>GFPRNAi
Gut
Malpighian tubule
Vkg-GFP DAPI
T
Fluorescence Intensity (A.U.)
No DSS
**
DSS
****
No KD
TubP> GFPRNAi
Piezo> GFPRNAi
Vkg-GFP KD